Proceedings of the Canadian Society for Mechanical Engineering International Congress 2021
CSME Congress 2021
June 27-30, 2021, Charlottetown, PE, Canada

Tube-Based Model Predictive Control of Small Satellite Systems with Uncertainty Dynamics

Elyse Hill[1], Mohammad Biglarbegian[1], S. Andrew Gadsden[1*]
[1]College of Engineering and Physical Sciences, University of Guelph, Guelph, Canada
*gadsden@uoguelph.ca

Abstract—In this paper, two tube-based model predictive control algorithms were developed using sliding mode control to regulate the attitude of a simulated CubeSat system. Incorporating sliding mode techniques increased the robustness of tube-based model predictive control by minimizing the uncertainty of the system in the presence of a disturbance. The proposed controllers' performances were evaluated against a traditional tube-based approach and measured in terms of root mean squared values on state errors and control efforts. Results indicate the effectiveness of the developed controllers over traditional tube-based methods for attitude control of small satellite systems, successfully extending this approach and opening an avenue for future development.

Model predictive control; small satellites; uncertainty dynamics; mathematical modelling

I. INTRODUCTION

Model predictive control (MPC) is a very successful control technique in which control effort is formulated in an open loop with respect to input and state constraints [1]. MPC has been praised for its remarkable control of complex, multivariable systems and its minimal conceptual complexity, leading to widespread application in the process industry [2]. Though powerful, MPC is dependent on model accuracy, and thus it breaks down in the presence of uncertainty, disturbances, and estimation or model error [3]. Because all real systems are plagued by disturbances, robust MPC (RMPC) methods have been developed to address system uncertainty [4]. A popular RMPC method is the tube-based MPC, which models system uncertainty as a 'tube' in which all state trajectories must reside [5]. This is enforced by tightening the state and input constraints such that they are satisfied for all possible realizations of the given disturbances [6].

A drawback to tube-based MPC is that its tightened constraints are designed on the worst possible effect of the disturbance, making its design conservative [7]. One possible solution is to link it to sliding mode control (SMC), a nonlinear controller which is inherently robust to uncertainties. This would allow the SMC to reject the disturbances present in the system in order to design a simpler MPC, an approach which has shown to be beneficial to the stability of linear MPC [7, 8, 9]. Reference [10] incorporated SMC by designing a controller on an uncertainty model, represented as the difference between the nominal and real systems. This was found to minimize overshoot, settling time, and steady state oscillations more than the methods outlined in [8] while maintaining system stability.

Minimizing performance specifications such as overshoot and steady state error is beneficial to attitude control, which requires fine, accurate pointing. NASA has identified attitude optimization with constraint accommodation as an area of focus [11]. In addition, control for small spacecraft, like smallsats or CubeSats, is a developing research area due to hardware limitations, actuation constraints, and susceptibility to disturbances [12, 13]. Current MPC applications on satellite systems have considered momentum management, satellite docking, and attitude maneuvering with respect to large angles and constrained attitude [14, 15, 16, 17, 18]. However, research using tube-based MPC has been limited to orbital maneuvering [19, 20, 21]. Indeed, of the handful of tube-based MPC applications, only [22] has been applied to not only attitude control but also to a small satellite. Though comprehensive, the methods used in [22] did not consider use of an SMC in the design, leaving room for investigation. Another work developed an explicit nonlinear model predictive control (eNMPC) based on an interacting multiple model (IMM) to tolerate actuator faults for a nonlinear spacecraft system [23].

This study seeks to expand the approach in [10] to develop schemes combining tube-based MPC and SMCs for CubeSat attitude control. Three control techniques will be implemented: tube-MPC, tube-MPC with SMC (MPC-SMC), and tube-MPC with boundary layer SMC (MPC-BLSMC). The schemes combining tube-MPC with sliding mode will use a hierarchical control scheme where the SMC samples at a faster rate than the MPC. Controller performance will be evaluated using root mean squared values on control effort and root mean squared error values on attitude. The goal of the controllers is regulation to the identity quaternion for a model CubeSat in the presence of a disturbance injected during the simulation.

The paper is organized as follows. The mathematical model of a satellite system is provided in Section II, followed by a summary of the controller strategies in Section III. The simulation setup and results are provided and described in Section IV, and the paper is then concluded

II. Mathematical Model of Satellite System

A. Satellite Kinematics and Dynamics

The attitude of a satellite can be represented by the quaternion, $\boldsymbol{q} = [q_1 \quad q_2 \quad q_3 \quad q_4]^T$, which has vector part $\boldsymbol{q}_{1:3}$ and scalar part q_4. This formation is used to avoid singularities that would be present using Euler angle notation. A rotation from the inertial frame to the body frame of a satellite can be described by a quaternion parameterized attitude matrix:

$$A(\boldsymbol{q}) = \left(q_4^2 - \left|\left|\boldsymbol{q}_{1:3}\right|\right|^2\right) I_3 + 2\boldsymbol{q}_{1:3}\boldsymbol{q}_{1:3}^T - 2q_4[\boldsymbol{q}_{1:3}\times] \quad (1)$$

where a skew-symmetric matrix $[\mathbf{y}\times]$ is described as

$$[\boldsymbol{y}\times] = \begin{bmatrix} 0 & -y_3 & y_2 \\ y_3 & 0 & -y_1 \\ -y_2 & y_1 & 0 \end{bmatrix}. \quad (2)$$

The kinematic and dynamic equations of a rigid body spacecraft with external disturbances can be defined as:

$$\dot{\boldsymbol{q}} = \frac{1}{2}\boldsymbol{\Omega}(\boldsymbol{\omega_b})\boldsymbol{q} \quad (3)$$

$$\dot{\boldsymbol{\omega_b}} = \boldsymbol{I_b^{-1}}[\boldsymbol{\tau_{ext}} + \boldsymbol{T_c} - [\boldsymbol{\omega_b}\times](\boldsymbol{I_b}\boldsymbol{\omega_b})] \quad (4)$$

where $\boldsymbol{\omega_b}=[\omega_x \quad \omega_y \quad \omega_z]$ is the angular velocity of the satellite body in the body frame, $\mathbf{I_b}$ is the moment of inertia of the satellite body represented a 3×3 matrix, $\boldsymbol{\tau_{ext}}$ is an external disturbance, $\mathbf{T_c}$ is the control torque input, and $\boldsymbol{\Omega(y)}$ equals

$$\boldsymbol{\Omega}(\boldsymbol{y}) = \begin{bmatrix} -[\boldsymbol{y}\times] & \boldsymbol{y} \\ -\boldsymbol{y}^T & 0 \end{bmatrix}. \quad (5)$$

To employ tube-based MPC, (3) and (4) must be expressed in linear state space form as:

$$\dot{\boldsymbol{x}} = \boldsymbol{A}\boldsymbol{x} + \boldsymbol{B}\boldsymbol{u} + \boldsymbol{B}\boldsymbol{w} \quad (6)$$

where the states are defined $\mathbf{x}=[\mathbf{q} \quad \boldsymbol{\omega_b}]^T$. The system is linearized around the equilibrium points of the identity quaternion, $\mathbf{I_q}=[0 \quad 0 \quad 0 \quad 1]^T$, and zero body angular velocity, $\boldsymbol{\omega_b}=[0 \quad 0 \quad 0]^T$. This produces:

$$\boldsymbol{A} = \begin{bmatrix} 0 & 0 & 0 & 0 & 0.5 & 0 & 0 \\ 0 & 0 & 0 & 0 & 0 & 0.5 & 0 \\ 0 & 0 & 0 & 0 & 0 & 0 & 0.5 \\ 0 & 0 & 0 & 0 & 0 & 0 & 0 \\ 0 & 0 & 0 & 0 & 0 & 0 & 0 \\ 0 & 0 & 0 & 0 & 0 & 0 & 0 \\ 0 & 0 & 0 & 0 & 0 & 0 & 0 \end{bmatrix} \quad (7)$$

$$\boldsymbol{B} = \begin{bmatrix} 0 & 0 & 0 \\ 0 & 0 & 0 \\ 0 & 0 & 0 \\ 0 & 0 & 0 \\ I_{b,xx}^{-1} & 0 & 0 \\ 0 & I_{b,yy}^{-1} & 0 \\ 0 & 0 & I_{b,zz}^{-1} \end{bmatrix} \quad (8)$$

$$\boldsymbol{u} = \boldsymbol{T_c} = [T_{c,x} \quad T_{c,y} \quad T_{c,z}]^T \quad (9)$$

$$\boldsymbol{w} = \boldsymbol{\tau_{ext}} = [\tau_{ext,x} \quad \tau_{ext,y} \quad \tau_{ext,z}]^T \quad (10)$$

As noted in [24], the linearized system is uncontrollable due to the scalar quaternion, q_4. To make the system controllable, this state is eliminated, reducing the state vector to $\tilde{x}=[q_{1:3} \quad \omega_b]^T$ and allowing q_4 to be determined by the quaternion constraint $\|q\|=1$. Note that $\tilde{x}$ is solely used for controller design purposes. Finally, to employ the control designs, (6) must be discretized with a sampling time, T, resulting in:

$$\boldsymbol{x}_{k+1} = (\boldsymbol{A}T + \boldsymbol{I}_{7\times7})\boldsymbol{x}_k + \boldsymbol{B}\boldsymbol{u}_k + \boldsymbol{B}\boldsymbol{w}_k \quad (11)$$

where $\mathbf{x}_k \in \mathbf{X} \in \mathbb{R}^n$, $\mathbf{u}_k \in \mathbf{U} \in \mathbb{R}^m$, $\mathbf{w}_k \in \mathbf{W} \in \mathbb{R}^m$, and $\mathbf{X}$, $\mathbf{U}$, $\mathbf{W}$ are compact sets containing their own origins and interiors representing constraints on the states, control inputs, and disturbances respectively.

B. Tracking Error

The tracking error for the system can be defined as the difference between the actual and desired values:

$$\boldsymbol{q_e} = \boldsymbol{q} \otimes \boldsymbol{q_d^{-1}} \quad (12)$$

$$\boldsymbol{\omega_e} = \boldsymbol{\omega_b} - \delta A \boldsymbol{\omega_d} \quad (13)$$

where $\mathbf{q}$ is the actual quaternion, $\mathbf{q_d}$ is the desired quaternion, $\boldsymbol{\omega_b}$ is the actual angular velocity of the body, $\boldsymbol{\omega_d}$ is the desired angular velocity of the body, and $\delta A = A(\mathbf{q})A_d^T(\mathbf{q_d})$ is the quaternion parameterized attitude error matrix that resolves the angular velocity error in body frame coordinates. The operator $\mathbf{q}\otimes$ represents:

$$\boldsymbol{q}\otimes = \begin{bmatrix} q_4\boldsymbol{I_3} - [\boldsymbol{q}_{1;3}\times] & \boldsymbol{q}_{1:3} \\ -\boldsymbol{q}_{1:3}^T & q_4 \end{bmatrix} \quad (14)$$

A tracking controller's goal is to follow a desired reference trajectory such that $q_{e,1:3} \to 0$ and $\omega_e \to 0$. Regulation is a special form of tracking where the goal is to drive the quaternion to I_q and drive the body angular velocities to zero [25].

III. Controller Strategies

A. Tube-based Model Predictive Control

A tube-based MPC can be formulated on the system of (11) by creating a nominal system model:

$$\bar{\boldsymbol{x}}_{k+1} = \boldsymbol{A}\bar{\boldsymbol{x}}_k + \boldsymbol{B}\bar{\boldsymbol{u}}_k \quad (15)$$

where $\bar{\mathbf{x}}_k$ is the nominal state and $\bar{\mathbf{u}}_k$ is the nominal control input. The control input is defined as $\bar{\mathbf{u}}_k=\mathbf{K_{LQR}}\bar{\mathbf{x}}_k$, where $\mathbf{K_{LQR}}$ is the LQR gain determined such that the closed loop system $\mathbf{A^{K_{LQR}}}=\mathbf{A}+\mathbf{BK_{LQR}}$ is stable. A robust invariant set, $\mathbf{S_0}$, represents a bounded neighborhood of the system trajectories perturbed by all disturbance sequences [5] and is formulated as

$$\boldsymbol{A^{K_{LQR}}X} \oplus \boldsymbol{W} \subseteq \boldsymbol{S_0} \quad (16)$$

where $\oplus$ is Minkowski set addition. As put forth in [5], if the controller $\mathbf{u}_k=\bar{\mathbf{u}}_k+\mathbf{K_{LQR}}(\mathbf{x}_k-\bar{\mathbf{x}}_k)$ is applied, then the nominal system satisfies the constraints

$$\bar{\boldsymbol{x}}_k \in \boldsymbol{X} \ominus \boldsymbol{S_0} \quad (17)$$

$$\bar{\boldsymbol{u}}_k \in \boldsymbol{U} \ominus \boldsymbol{K_{LQR}}\boldsymbol{S_0} \quad (18)$$

where $\ominus$ is Minkowski set subtraction, and the state of the real system tracks the nominal system. An alternative version of this formulation was proposed in [26], defining the controller as $\mathbf{u}_k=\bar{\mathbf{u}}_k+\mathbf{K_{LQR}}(\mathbf{x}_k-\bar{\mathbf{x}}_0)$, where $\bar{\mathbf{x}}_0$ is the initial state of the nominal

system that is redefined as a parameter of the MPC optimization problem. The optimization problem is

$$\begin{aligned} \min_{\bar{\boldsymbol{u}}_{(\cdot)},\bar{\boldsymbol{x}}_0} & \sum_{j=0}^{N-1} l(\bar{\boldsymbol{x}}_j, \bar{\boldsymbol{u}}_j) + V_f(\bar{\boldsymbol{x}}_N) \\ \text{subject to } & \bar{\boldsymbol{x}}_{k+1} = \boldsymbol{A}\bar{\boldsymbol{x}}_k + \boldsymbol{B}\bar{\boldsymbol{u}}_k, \\ & \bar{\boldsymbol{x}}_k \in \boldsymbol{X} \ominus \boldsymbol{S_0}, \\ & \bar{\boldsymbol{u}}_k \in \boldsymbol{U} \ominus \boldsymbol{K_{LQR}}\boldsymbol{S_0}, \\ & \boldsymbol{x_0} \in \bar{\boldsymbol{x}}_0 \oplus \boldsymbol{S_0}, \\ & \bar{\boldsymbol{x}}_N \in \boldsymbol{X_f} \ominus \boldsymbol{S_0} \end{aligned} \tag{19}$$

where N is the prediction horizon, $\mathbf{X_f}$ is the terminal constraint set, $l(\cdot)=\|\bar{\mathbf{x}}_k-\mathbf{x_{ref}}\|_{\mathbf{Q}}^2+\|\bar{\mathbf{u}}_k\|_{\mathbf{R}}^2$ is the stage cost between the desired trajectory and the predicted states, and $V_f(\cdot)= \|\bar{\mathbf{x}}_N-\mathbf{x_{ref}}\|_{\mathbf{P}}^2$ is the terminal cost function. The operation $\|\cdot\|_{\mathbf{W}}^2$ represents the Euclidean norm of a vector weighted by a matrix $\mathbf{W}$. The matrices $\mathbf{Q}\in\mathbb{R}^{n\times n}$, $\mathbf{R}\in\mathbb{R}^{m\times m}$, $\mathbf{P}\in\mathbb{R}^{n\times n}$ are positive definite weighting matrices.

B. Uncertainty Model Compensation

As seen in [8] and [7], a two-level control design can be established for the control input of an MPC

$$\boldsymbol{u} = \bar{\boldsymbol{u}} + \boldsymbol{u}_{SMC} \tag{20}$$

where $\bar{\mathbf{u}}$ is a higher-level controller based on MPC and $\mathbf{u}_{SMC}$ is a lower-level controller based on a sliding mode design. From [10], $\mathbf{u}_{SMC}$ can be designed to stabilize the system uncertainty, $\mathbf{z}$, expressed as the difference between the real and nominal systems:

$$\boldsymbol{z} = \boldsymbol{x} - \bar{\boldsymbol{x}} \tag{21}$$

The dynamics of this model are assumed second order:

$$\ddot{\boldsymbol{z}} = h(\boldsymbol{z}) + \boldsymbol{u}_{SMC} \tag{22}$$

where $h(\mathbf{z})$ is the unknown, nonlinear dynamics of the system, $\mathbf{z}$ is the output of the system, and $\mathbf{u}_{SMC}$ is the control input. The dynamics are upper bounded by H as:

$$|h| \leq H \tag{23}$$

The tracking error of these dynamics is defined as:

$$\boldsymbol{z_e} = \boldsymbol{z} - \boldsymbol{z_d} \tag{24}$$

where $\mathbf{z_e}$ is the tracking error and $\mathbf{z_d}$ is the desired uncertainty.

The goal of this controller is to drive the output, z, to zero. With regards to satellite dynamics, the desired values of z and its derivatives can be written as $\boldsymbol{z_d} = \boldsymbol{I_q}$ and $\dot{z}_d=\ddot{z}_d=0$. The error dynamics of the spacecraft system can be exploited to define the uncertainty states as:

$$\boldsymbol{z} = \boldsymbol{q_{e,1:3}} = \boldsymbol{x_{1:4}} \otimes \bar{\boldsymbol{x}}_{\boldsymbol{1:4}}^{-\boldsymbol{1}} \tag{25}$$

$$\dot{\boldsymbol{z}} = \boldsymbol{\omega_e} = \boldsymbol{x_{5:7}} - \bar{\boldsymbol{x}}_{\boldsymbol{5:7}} \tag{26}$$

A sliding mode controller can be designed with the sliding surface:

$$\boldsymbol{S} = \left(\frac{d}{dt} + \lambda\right)\boldsymbol{z_e} = \dot{\boldsymbol{z}}_{\boldsymbol{e}} + \boldsymbol{\lambda}\boldsymbol{z_e} \tag{27}$$

where $\boldsymbol{\lambda}$ is a positive 3×3 diagonal matrix. Differentiating (27) with respect to time results in:

$$\dot{\boldsymbol{S}} = \ddot{\boldsymbol{z}}_{\boldsymbol{e}} + \boldsymbol{\lambda}\dot{\boldsymbol{z}}_{\boldsymbol{e}} \tag{28}$$

To solve for the estimated control torque, $\hat{\mathbf{u}}_{SMC}$, (26) is plugged into (28), which is then set to zero, producing:

$$\hat{\boldsymbol{u}}_{SMC} = -\hat{h}(\boldsymbol{z}) + \ddot{\boldsymbol{z}}_{\boldsymbol{d}} - \boldsymbol{\lambda}\dot{\boldsymbol{z}}_{\boldsymbol{e}} \tag{29}$$

The total input, $\mathbf{u}_{SMC}$, is found by adding a discontinuous term across the sliding surface:

$$\boldsymbol{u}_{SMC} = \hat{\boldsymbol{u}}_{SMC} - \boldsymbol{K}sign(\boldsymbol{S}) \tag{30}$$

where $\mathbf{K}$ is a positive 3×3 diagonal matrix. The discontinuous term is designed to eliminate the function $h(\mathbf{z})$ as it is unknown, therefore ensuring $\dot{\mathbf{S}}=\mathbf{0}$. In this paper, two sliding mode designs are considered for the uncertainty model: traditional sliding mode control (SMC) and boundary layer sliding mode control (BLSMC). SMC design is represented by (30), but BLSMC expands on (30) by altering the discontinuous term:

$$\boldsymbol{u}_{BLSMC} = \hat{\boldsymbol{u}}_{SMC} - \bar{\boldsymbol{K}}sat\left(\frac{\boldsymbol{S}}{\boldsymbol{\phi}}\right) \tag{31}$$

where $\bar{\mathbf{K}}=\mathbf{K(z)}-\dot{\boldsymbol{\phi}}$, $\boldsymbol{\phi}$ is a positive 3×1 vector representing the boundary layer thickness, $\mathbf{K}(z)$ is the gain for the real system, and the $sat(\cdot)$ function is defined as:

$$sat\left(\frac{\boldsymbol{S}}{\boldsymbol{\phi}}\right) = \frac{\boldsymbol{S}}{\boldsymbol{\phi}} if \left|\frac{\boldsymbol{S}}{\boldsymbol{\phi}}\right| \leq 1$$

$$sat\left(\frac{\boldsymbol{S}}{\boldsymbol{\phi}}\right) = sign(\boldsymbol{S}) \; otherwise \tag{32}$$

The value for $\dot{\boldsymbol{\phi}}$ is determined by:

$$\dot{\boldsymbol{\phi}} + \boldsymbol{\lambda}\boldsymbol{\phi} = \boldsymbol{K}(\boldsymbol{z_d}) \tag{33}$$

where $\mathbf{K}(\mathbf{z_d})$ is the gain for the uncertain system. The standard proofs of stability for both sliding mode controllers may be found using Lyapunov theory. The proofs have been omitted from this conference paper due to space constraints, but will be included in a journal publication.

IV. Simulations and Results

In this paper we simulated an example from [25], which performed a regulation attitude maneuver. The simulation is implemented in MATLAB® using CasADi [27]. System parameters and initial conditions are provided in Tab. 1. The state and input constraints are selected as

$$|\tilde{\boldsymbol{x}}| \leq [1 \quad 1 \quad 1 \quad 5 \quad 5 \quad 5]^T \tag{34}$$

$$|\boldsymbol{u}| \leq [0.408 \quad 0.408 \quad 0.408]^T Nm \tag{35}$$

Values for the inertia matrix and the input constraints were based on those found in [28] for a 3U Cubesat. The MPC and SMC operate as a hierarchical control scheme, resulting in different sampling rates. The sampling time of the MPC is set to T=1s with a prediction horizon of N=14 and the sampling time of the SMC controllers is set to T=0.1s. The simulation time is set to t=20min . An external torque $\boldsymbol{\tau_{ext}}=[0.05\sin(0.05t) \quad 0.03 \quad 0.05\cos(0.05t)]^T$ is applied at t=6.5min to evaluate the control methods in the presence of disturbances.

Controller performance was evaluated using the root mean square (RMS) error for the states ($\mathbf{x}_{RMSE}$) and the RMS value for the control effort ($\mathbf{u}_{RMS}$). Tabs. 2 and 3 present these values for each strategy while Figs. 1 and 2 display the attitude maneuvers and Fig 3 displays the resulting control efforts, respectively. As seen from the quaternion response and body angular velocities, MPC with either sliding mode control design settles faster and is more robust to the disturbance than the MPC. Both MPC-SMC and MPC-BLSMC have smaller magnitudes of error and recover near instantaneously to the disturbance across all states. In contrast, MPC takes ~1.5min to

stabilize attitude and ~1min to stabilize angular velocity. Numerically, MPC-SMC and MPC-BLSMC are found to perform nearly identically, given their $\mathbf{x}_{RMSE}$ values, while both outperform pure MPC.

TABLE I. SYSTEM PARAMETERS

Parameter	Value
$\mathbf{I_b}$	$\begin{bmatrix}0.0056 & 0 & 0\\ 0 & 0.026 & 0\\ 0 & 0 & 0.0026\end{bmatrix}$ kgm^2
$\mathbf{q_0}$	$[0.2 \quad 0.3 \quad 0.4 \quad 0.8]^T$
$\boldsymbol{\omega_{b,0}}$	$[0.01 \quad 0.01 \quad 0.01]^T$rad/s
MPC Gains and Weights	
Parameter	**Value**
$\mathbf{K_{LQR}}$	$\begin{bmatrix}-0.004 & 0 & 0 & -0.008 & 0 & 0\\ 0 & -0.2 & 0 & 0 & -0.04 & 0\\ 0 & 0 & -0.002 & 0 & 0 & -0.004\end{bmatrix}$
Q	$\begin{bmatrix}1&0&0&0&0&0\\0&1&0&0&0&0\\0&0&1&0&0&0\\0&0&0&1&0&0\\0&0&0&0&1&0\\0&0&0&0&0&1\end{bmatrix}$
R	$\begin{bmatrix}10&0&0\\0&10&0\\0&0&10\end{bmatrix}$
P	$\begin{bmatrix}3.56&0&0&1.28&0&0\\0&3.56&0&0&1.28&0\\0&0&3.56&0&0&1.28\\1.28&0&0&1.64&0&0\\0&1.28&0&0&1.65&0\\0&0&1.28&0&0&1.64\end{bmatrix}$
SMC Gains	
Parameter	**Value**
$\boldsymbol{\lambda}$,	$\begin{bmatrix}4\times10^{-5}&0&0\\0&2\times10^{-3}&0\\0&0&2\times10^{-5}\end{bmatrix}$
K	$\begin{bmatrix}8\times10^{-6}&0&0\\0&4\times10^{-5}&0\\0&0&4\times10^{-6}\end{bmatrix}$
BLSMC Gains	
Parameter	**Value**
$\boldsymbol{\lambda}$,	$\begin{bmatrix}4\times10^{-3}&0&0\\0&2\times10^{-1}&0\\0&0&2\times10^{-3}\end{bmatrix}$
$\mathbf{K(z)=K(z_d)}$,	$\begin{bmatrix}8\times10^{-1}&0&0\\0&4&0\\0&0&4\times10^{-1}\end{bmatrix}$
$\boldsymbol{\phi}$	$[1\times10^{-5} \quad 1\times10^{-5} \quad 1\times10^{-5}]^T$

TABLE II. $\mathbf{x}_{RMSE}$ VALUES

	Attitude Error (Quaternion)				Angular Velocity Error (rad/s)		
Controller	$\mathbf{q_1}$	$\mathbf{q_2}$	$\mathbf{q_3}$	$\mathbf{q_4}$	$\boldsymbol{\omega_x}$	$\boldsymbol{\omega_y}$	$\boldsymbol{\omega_z}$
Tube MPC	0.061	0.056	0.074	0.99	0.053	0.022	0.030
MPC-SMC	0.013	0.016	0.021	1.0	0.016	0.008	0.011
MPC-BLSMC	0.016	0.017	0.022	1.0	0.015	0.007	0.010

TABLE III. $\mathbf{u}_{RMS}$ VALUES

	Torque (Nm)		
Controller	$\mathbf{T_x}$	$\mathbf{T_y}$	$\mathbf{T_z}$
Tube MPC	4.32×10^{-4}	4.51×10^{-4}	6.64×10^{-5}
MPC-SMC	2.01×10^{-4}	2.35×10^{-4}	4.03×10^{-5}
MPC-BLSMC	1.64×10^{-4}	1.67×10^{-4}	3.13×10^{-5}

TABLE IV. $\mathbf{z}_{RMSE}$ VALUES

	Attitude Error (Quaternion)			
Controller	$\mathbf{q_1}$	$\mathbf{q_2}$	$\mathbf{q_3}$	$\mathbf{q_4}$
MPC-SMC	0.0057	0.0042	0.0057	1.0
MPC-BLSMC	0.0054	0.004	0.0054	1.0

Examining Fig. 3 highlights the benefit of MPC-BLSMC over MPC-SMC. Each figure has a zoomed in view of the control torque during its recovery from the disturbance. While both MPC-SMC and MPC-BLSMC immediately recovered from the disturbance, MPC-SMC has a distinct amount of chatter that is not found in the MPC-BLSMC. This is consistent across all axes and is most significant in the Y-Axis (Fig. 3b). MPC-BLSMC outperforms both controllers in terms of u_{RMS} values as well, being significantly smaller than MPC torques and slightly smaller than MPC-SMC torques. An additional set of RMSE values, z_{RMSE}, are presented in Tab. 4, which displays the error values for the uncertainty states used in the sliding mode controllers. As shown, both controllers drive the uncertainty towards I_q for the quaternion states, indicating their ability to minimize the difference between the nominal and disturbance-perturbed systems.

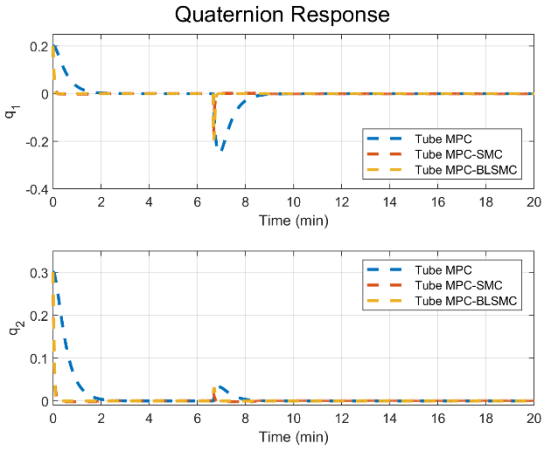

(a)

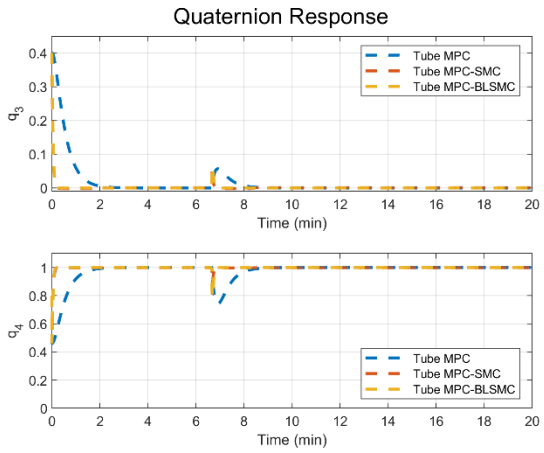

(b)

Figure 1. Quaternion Response on CubeSat

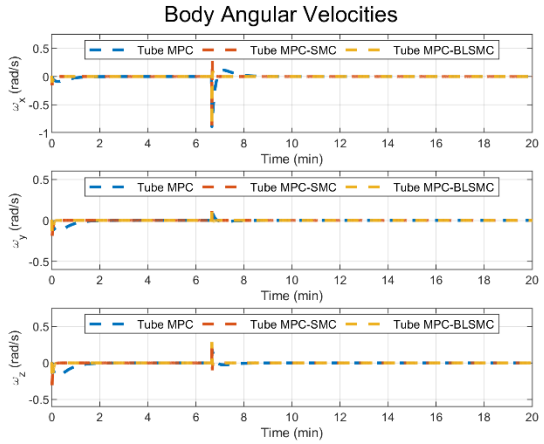

Figure 2. Body Angular Velocity Response of CubeSat

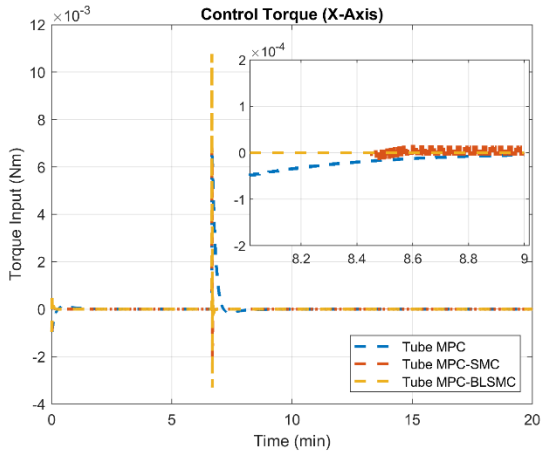

(a)

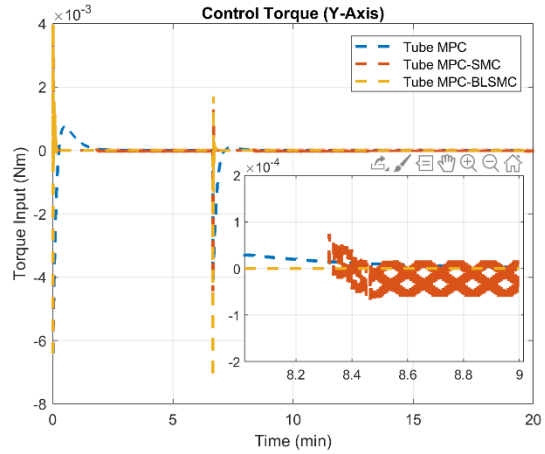

(b)

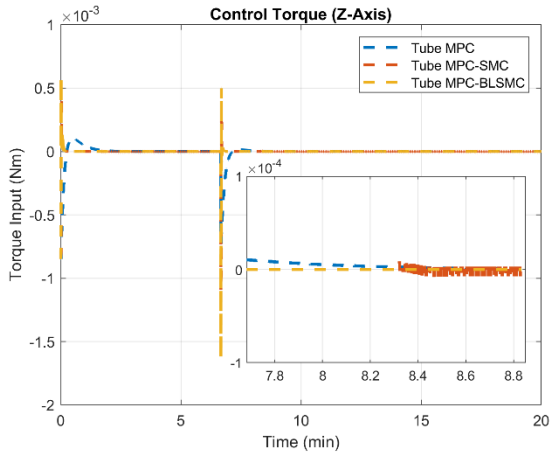

(c)

Figure 3. Control Input Signals for CubeSat along (a) X-Axis (b) Y-Axis (c) Z-Axis

V. Conclusion

This paper developed two tube-MPC controllers for the attitude control of a simulated CubeSat using the sliding mode control techniques of SMC and BLSMC. Designing on the uncertainty between the real and nominal systems minimized the system error in the presence of a disturbance, thereby increasing robustness. While the sliding mode controllers seemed to perform identically, MPC-BLSMC experience significantly less chatter in its control efforts, which is important for practical applications. Though a simplified example, the main contributions of this paper are: developing the advantageous tube-MPC/SMC design and validating its superiority against traditional tube-MPC for attitude control of a CubeSat system. These results lay the foundation for future investigation such as: simulation on a tracking problem, incorporation of real-world spacecraft disturbances over longer durations, and application to an experimental CubeSat.

REFERENCES

[1] D. Q. Mayne, "Model predictive control: recent developments and future promise," *Automatica,* vol. 50, no. 12, pp. 2967-2986, 2014.

[2] M. G. Forbes, R. S. Patwardhan, H. Hamadah and R. B. Gopaluni, "Model predictive control in industry: Challenges and opportunities," *IFAC-PapersOnLine,* vol. 28, no. 8, pp. 531-538, 2015.

[3] D. Q. Mayne, E. C. Kerrigan and P. Falugi, "Robust model predictive control: advantages and disadvantages of tube-based methods," *IFAC Proceedings Volumes,* vol. 44, no. 1, pp. 191-196, 2011.

[4] R. S. Gesser, D. M. Lima and J. E. Normey-Rico, "Robust Model Predictive Control: Implementation Issues with Comparative Analysis," *IFAC-PapersOnLine,* vol. 51, no. 25, pp. 478-483, 2018.

[5] J. B. Rawlings, D. Q. Mayne and M. M. Diehl, Model Predictive Control: Theory, Computation, and Design, 2nd ed., Santa Barbara, California: Nob Hill Publishing, 2019.

[6] S. Rakovic, A. R. Teel, D. Q. Mayne and A. A., "Simple Robust Control Invariant Tubes for Some Classes of Nonlinear Discrete Time Systems," in *Proceedings of the 45th IEEE Conference on Decision and Control*, San Diego, 2006.

[7] M. Rubagotti, D. M. Raimondo and A. Ferrara, "Robust model predictive control with integral sliding mode in continuous-time sampled-data nonlinear systems," *IEEE Transactions on Automatic Control,* vol. 56, no. 3, pp. 556-570, 2011.

[8] G. P. Incremona, A. Ferrara and L. Magni, "Hierarchical model predictive/sliding mode control of nonlinear constrained uncertain systems," *International Federation of Automatic Control,* vol. 48, no. 23, pp. 102-109, 2015.

[9] G. P. Incremona, A. Ferrara and L. Magni, "MPC for robot manipulators with integral sliding modes generation," *IEEE/ASME Transactions on Mechatronics,* vol. 22, no. 3, pp. 1299-1307, 2017.

[10] E. Kayacan and J. Peschel, "Robust model predictive control of systems by modeling mismatched uncertainty," *International Federation of Automatic Control,* vol. 49, no. 18, pp. 265-269, 2016.

[11] N. A. a. S. Administration, "2020 NASA Technology Taxonomy," 2020.

[12] F. Lamnabhi-Lagarrigue, A. Annaswamy, S. Engell, A. Isaksson, P. Khargonekar, R. M. Murray, H. Nijmeijer, T. Samad, D. Tilbury and P. Van den Hof, "Systems & Control for the future of humanity, research agenda: Current and future roles, impact and grand challenges," *Annual Reviews in Control,* vol. 43, pp. 1-64, 2017.

[13] A. Newton, E. Hill, S. A. Gadsden, M. Biglarbegian and S. Yang, "Investigating Reaction Wheel Configuration and Control Law Pairings for CubeSats in the Presence of Faults," in *Progress in Canadian Mechanical Engineering (CSME)*, Charlottetown, PEI, 2020.

[14] D. Y. Lee, R. Gupta, U. V. Kalabic, S. Di Cairano, A. M. Bloch, J. W. Cutler and I. V. Kolmanovsky, "Constrained attitude maneuvering of a spacecraft with reaction wheel assembly by Nonlinear Model Predictive Control," in *Proceedings of the American Control Conference*, Boston, 2016.

[15] R. Sutherland, I. Kolmanovsky and A. R. Girard, "Attitude Control of a 2U Cubesat by Magnetic and Air Drag Torques," *IEEE Transactions on Control Systems Technology,* vol. 27, no. 3, pp. 1047-1059, 2019.

[16] A. Sakamoto, Y. Ikeda, I. Yamaguchi and T. Kida, "Nonlinear model predictive control for large angle attitude maneuver of spacecraft with RW and RCS," in *2016 IEEE 55th Conference on Decision and Control, CDC 2016*, 2016.

[17] A. Walsh, S. Di Cairano and A. Weiss, "MPC for coupled station keeping, attitude control, and momentum management of low-thrust geostationary satellites," in *Proceedings of the American Control Conference*, 2016.

[18] R. J. Caverly, S. Di Cairano and A. Weiss, "Split-Horizon MPC for Coupled Station Keeping, Attitude Control, and Momentum Management of GEO Satellites using Electric Propulsion," in *Proceedings of the American Control Conference*, 2018.

[19] C. Buckner and R. Lampariello, "Tube-Based Model Predictive Control for the Approach Maneuver of a Spacecraft to a Free-Tumbling Target Satellite," in *Proceedings of the American Control Conference*, 2018.

[20] M. Mammarella, E. Capello, H. Park, G. Guglieria and M. Romano, "Tube-based robust model predictive control for spacecraft proximity operations in the presence of persistent disturbance," *Aerospace Science and Technology,* vol. 77, pp. 585-594, 2018.

[21] M. Martina, E. Capello, H. Park, G. Guglieri and M. Romano, "Spacecraft Proximity Operations via Tube-based Robust Model Predictive Control with Additive Disturbances," in *68th International Astronautical Congress*, Adelaide, 2017.

[22] M. Mammarella, D. Y. Lee, H. Park, E. Capello, M. Dentis and G. Guglieri, "Attitude control of a small spacecraft via tube-based model predictive control," *Journal of Spacecraft and Rockets,* vol. 56, no. 6, pp. 1662-1679, 2019.

[23] E. Hill, S. A. Gadsden and M. Biglarbegian, "Explicit Nonlinear MPC for Fault Tolerance using Interacting Multiple Models," *IEEE Transactions on Aerospace and Electronic Systems,* 2021.

[24] Ø. Hegrenæs, J. T. Gravdahl and P. Tøndel, "Spacecraft attitude control using explicit model predictive control," *Automatica,* vol. 41, no. 12, pp. 2107-2114, 2005.

[25] F. L. Markley and J. Crassidis, Space Technology Library Fundamentals of Spacecraft Attitude Determination and Control, New York: Springer, 2014.

[26] D. Mayne, M. Seron and S. Rakovic, "Robust model predictive control of constrainted linear systems with bounded disturbances," *Automatica,* vol. 41, no. 2, pp. 219-224, 2005.

[27] J. A. Andersson, J. Gillis, G. Horn, J. E. Rawlings and M. Diehl, "CasADi: A software framework for nonlinear optimization and optimal control," *Mathematical Programming Computation,* vol. 11, no. 1, pp. 1-36, 2019.

[28] L. Jonsson, "Simulations of Satellite Attitude Maneuvers - Detumbling and Pointing," 2019.

[29] M. B. Saltık, L. Özkan, J. H. Ludlage, S. Weiland and P. M. Van den Hof, "An outlook on robust model predictive control algorithms: Reflections on performance and computational aspects," *Journal of Process Control,* vol. 61, pp. 77-102, 2018.

[30] Z. Wan and M. V. Kothare, "Efficient robust constrained model predictive control with a time varying terminal constraint set," *Systems & Control Letters,* vol. 48, no. 5, pp. 375-383, 2003.

[31] S. V. Raković, B. Kouvaritakis, R. Findeisen and M. Cannon, "Homothetic tube model predictive control," *Automatica,* vol. 48, no. 8, pp. 1631-1638, 2012.

[32] S. V. Rakovic, B. Kouvaritakis, M. Cannon, C. Panos and R. Findeisen, "Parameterized Tube Model Predictive Control," *IEEE Transactions on Automatic Control,* vol. 57, no. 11, pp. 2746-2761, 2012.

[33] B. Kouvaritakis, M. Cannon and R. Yadlin, "On the centres and scalings of robust and stochastic tubes," in *UKACC International Conference on Control 2010*, Coventry, 2010.

[34] Y. Kim, X. Zhang, J. Guanetti and F. Borrelli, "Robust Model Predictive Control with Adjustable Uncertainty Sets," in *2018 IEEE Conference on Decision and Control (CDC)*, Miami Beach, 2018.